NRC·CNRC

NRC Publications Archive
Archives des publications du CNRC

Accelerated conditioning for a proton exchange membrane fuel cell

Yuan, Xiao-Zi; Sun, Jian Colin; Wang, Haijiang; Li, Hui

This publication could be one of several versions: author's original, accepted manuscript or the publisher's version. / La version de cette publication peut être l'une des suivantes : la version prépublication de l'auteur, la version acceptée du manuscrit ou la version de l'éditeur.
For the publisher's version, please access the DOI link below./ Pour consulter la version de l'éditeur, utilisez le lien DOI ci-dessous.

Publisher's version / Version de l'éditeur:
https://doi.org/10.1016/j.jpowsour.2012.01.039
Journal of Power Sources, 205, pp. 340-344, 2012-01-10

NRC Publications Record / Notice d'Archives des publications de CNRC:
https://nrc-publications.canada.ca/eng/view/object/?id=24ca7dbb-bdda-4a21-90ff-f7b32aca251f
https://publications-cnrc.canada.ca/fra/voir/objet/?id=24ca7dbb-bdda-4a21-90ff-f7b32aca251f

Access and use of this website and the material on it are subject to the Terms and Conditions set forth at https://nrc-publications.canada.ca/eng/copyright
READ THESE TERMS AND CONDITIONS CAREFULLY BEFORE USING THIS WEBSITE.

L'accès à ce site Web et l'utilisation de son contenu sont assujettis aux conditions présentées dans le site https://publications-cnrc.canada.ca/fra/droits
LISEZ CES CONDITIONS ATTENTIVEMENT AVANT D'UTILISER CE SITE WEB.

Questions? Contact the NRC Publications Archive team at PublicationsArchive-ArchivesPublications@nrc-cnrc.gc.ca. If you wish to email the authors directly, please see the first page of the publication for their contact information.

Vous avez des questions? Nous pouvons vous aider. Pour communiquer directement avec un auteur, consultez la première page de la revue dans laquelle son article a été publié afin de trouver ses coordonnées. Si vous n'arrivez pas à les repérer, communiquez avec nous à PublicationsArchive-ArchivesPublications@nrc-cnrc.gc.ca.

National Research Council Canada | Conseil national de recherches Canada

Canada

Journal of Power Sources 205 (2012) 340–344

Contents lists available at SciVerse ScienceDirect

Journal of Power Sources

journal homepage: www.elsevier.com/locate/jpowsour

Short communication

Accelerated conditioning for a proton exchange membrane fuel cell

Xiao-Zi Yuan*, Jian Colin Sun, Haijiang Wang**, Hui Li

Institute for Fuel Cell Innovation, National Research Council Canada, 4250 Wesbrook Mall, Vancouver, BC, Canada V6T 1W5

ARTICLE INFO

Article history:
Received 26 October 2011
Received in revised form
21 December 2011
Accepted 1 January 2012
Available online 10 January 2012

Keywords:
Conditioning
Pre-conditioning
Activating
Commissioning
Break-in

ABSTRACT

A conditioning process is usually needed for a newly fabricated proton exchange membrane (PEM) fuel cell to be activated. Depending on the membrane electrode assemblies, this process can take hours and even days to complete. To provide for accelerated conditioning techniques that can complete the process in a short time, this paper compares various reported methods to condition a PEM single cell. The major objectives are to identify accelerated conditioning approaches that can significantly reduce the conditioning duration for the existing conditioning regime in an operationally easy manner, and to understand the fundamental principles that govern accelerated conditioning. Various effects investigated include temperature, cycling steps, and cycling frequencies. Other techniques, such as short circuiting, hydrogen pumping, and hot water circulation, are also discussed. For each technique, measurements are taken using electrochemical impedance spectroscopy (EIS), cyclic voltammetry (CV), and linear sweep voltammetry (LSV).

Crown Copyright © 2012 Published by Elsevier B.V. All rights reserved.

1. Introduction

A conditioning process is usually needed for a newly fabricated polymer electrolyte membrane (PEM) fuel cell to be activated [1]. Through this process, also called break-in, commissioning, or incubation, the new cell can reach its best performance. Typically, during this break-in period the cell performance increases gradually, then reaches a plateau without further increase. Depending on the membrane electrode assemblies (MEAs), this process can take hours and even days to complete. An ideal scenario is not only to have the highest possible power density after the break-in procedure, but also to minimize the activation completion time [2,3].

Various approaches have been investigated to maximize fuel cell performance and shorten the electrode activation time. On-line techniques explored include current control [5,6], potential control [7,8], temperature control [9–11], hydrogen pumping [4,12], CO stripping [13], and air braking [14,15]. Off-line methods include electrochemical conditioning of the MEA [16], and steaming or boiling the electrode [17]. The US Fuel Cell Council (USFCC) has even established cell break-in protocols to standardize the process [18]. However, no standard measurement has been established to determine the effectiveness of a break-in or conditioning procedure. Murthy et al. [3] recommended monitoring a fuel cell's output current density at 0.6 V and recording it as a function of time during the application of a given conditioning procedure.

Compared with fuel cell durability studies, research on fuel cell conditioning is relatively limited. In most cases, procedures are given and results are presented without digging further into the mechanisms. As a result, the reports contain more hypotheses than facts. Most mechanisms proposed are hypothetical because they lack direct experimental support or concrete experimental verification. A systematic investigation of conditioning and its mechanisms is still required. To this end, the present paper aims to identify accelerated conditioning approaches that can significantly reduce the conditioning duration for an existing conditioning regime, with easy operational conditions, and to understand the fundamental principles that govern accelerated conditioning. Various effects investigated include temperature, cycling steps, and cycling frequencies. Other techniques, such as short circuiting, hydrogen pumping, and hot water circulation, are also discussed.

2. Experimental

2.1. Accelerated conditioning

The PEM fuel cell had an active area of 50 cm^2. All the experiments were carried out using Gore 57 catalyst coated membranes (CCMs). To ensure instant temperature control in the cell, all of the gases and water could be operated to bypass the cell through three-way valves.

The baseline data was obtained by drawing the current at a constant voltage of 0.6 V. Once the initial set points were reached (70 °C, with 100% relative humidity (RH) on both sides), the cell was

* Corresponding author. Tel.: +1 604 221 3000x5576; fax: +1 604 221 3001.
** Corresponding author. Tel.: +1 604 221 3038; fax: +1 604 221 3001.
E-mail addresses: xiao-zi.yuan@nrc.gc.ca (X.-Z. Yuan), haijiang.wang@nrc.gc.ca (H. Wang).

0378-7753/$ – see front matter. Crown Copyright © 2012 Published by Elsevier B.V. All rights reserved.
doi:10.1016/j.jpowsour.2012.01.039

connected to the system. After 6 h of operation at 0.6 V, EIS, CV, and LSV were measured. Then cell operation was continued at 0.6 V until there was no further performance improvement, at which point EIS, CV, and LSV measurements were taken again.

Factors that affect conditioning were chosen based on ease of operation and the effectiveness of the method, and included temperature, cycling steps, and cycling frequencies. Assessment of temperature effects was performed at 50 °C, 70 °C (baseline), and 90 °C, at a constant voltage of 0.6 V and 100%RH on both sides for 6 h. To determine the effect of cycling steps, three experiments were carried out: (1) the cell was cycled between 0.6 V and 0.3 V, with each set point held for 60 s, and the cycle was repeated for 6 h. (2) The cell was cycled between 0.6 V, 0.3 V, and OCV, with each set point held for 60 s, and the cycle was repeated for 6 h. (3) The cell was cycled in a sequence of potential cycling steps, as follows:

(i) Cell voltage was decreased from 0.9 V to 0.2 V and maintained for 60 s at each decrease of 0.1 V.
(ii) Cell voltage was maintained at 0.1 V for 60 s.
(iii) Cell voltage was increased from 0.2 V to 0.9 V and maintained for 60 s at each increase of 0.1 V.
(iv) The above three steps were repeated for 6 h.

To investigate the influence of cycling frequency, two other tests were added: the cell was cycled between 0.6 V and 0.3 V, with each set point held for (1) 5 min or (2) 20 s. The conditions of all these tests were the same as for the baseline. Each conditioning process was performed for 6 h, and EIS, CV, and LSV were measured immediately afterward.

Other techniques investigated in this paper included short circuit, hot water circulation, and hydrogen evolution/hydrogen pumping. The procedures for short circuit were as follows. The anode and the cathode were connected to short the cell, with a low flow rate for 1 min and a high flow rate for 3 min. This process was repeated for 0.5 h. At the end of this process, hydrogen was supplied at a minimum rate and oxygen supply was stopped. When the cell voltage was below 0.1 V, the hydrogen supply was stopped. For hot water circulation, hot water (80 °C) was circulated for both anode and cathode for 0.5 h, and then the electrochemical performances were measured. For hydrogen evolution/hydrogen pumping, air at the cathode side was replaced by nitrogen, while the anode side was fed with pure hydrogen. An external power supply was used to generate a current density of ca. 200 mA cm^{-2} through the cell, with hydrogen being oxidized at the anode; the protons were transported through the membrane to the cathode, where they were reduced. The procedure was continued for 30 min.

2.2. Electrochemical techniques

To assess the effectiveness of activation and to understand the underlying principles, EIS, CV, and LSV were measured after each conditioning process. A Solartron SI-1260 Impedance/Gain-Phase analyzer and a Solartron SI-1287 Electrochemical Interface were used for EIS testing at a current of 36 A over the frequency range of 10 kHz to 0.1 Hz.

Prior to the CV and LSV tests, the air supply was switched to nitrogen and the system was run at OCV with H_2 min flow (0.5 l min^{-1}) and N_2 min flow (2 l min^{-1}) until steady potential was achieved. In situ CV was performed on the fuel cell using the Solartron SI-1287 Electrochemical Interface to compare the relative electrochemical surface area (ECSA). To avoid possible degradation from carbon support oxidation induced by high potentials, the cell was cycled between 0.05 and 0.8 V on the cathode vs. reversible hydrogen electrode (RHE) at a scan rate of 50 mV s^{-1}.

The gas permeability or crossover through the membrane was assessed using LSV to measure the limiting oxidation current densities of the crossover hydrogen. For LSV measurement, all the operating conditions for the fuel cell were the same as in the CV test, except for a linear potential scan from 0 to 0.5 V (vs. RHE) on the cathode at a scan rate of 5 mV s^{-1}.

For each experiment, the output current density of the cell at 0.6 V was monitored and extracted from the data as a function of time.

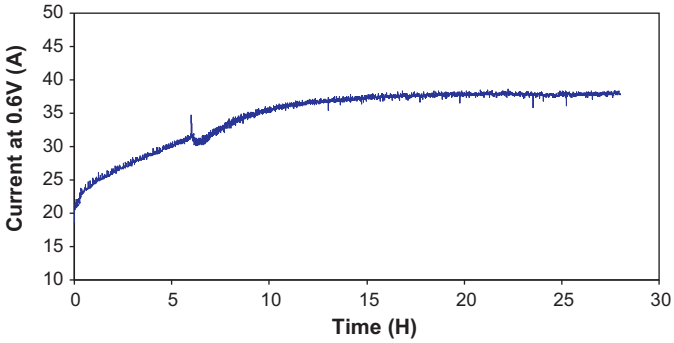

Fig. 1. Time dependence of current at 0.6 V for the baseline.

3. Results and discussion

3.1. Baseline

The baseline data was obtained by drawing the current at a constant voltage of 0.6 V and at 70 °C for 100 h. Fig. 1 shows the time dependence of current at 0.6 V during baseline conditioning (note that the figure presents only the first 28 h). As can be seen, the current increases with time for about 20 h, with the greatest increase occurring at the very beginning. After 20 h, no further performance improvement is observed. After 6, 28, and 100 h of operation at 0.6 V, EIS, CV, and LSV were measured (shown in Figs. 2–4, respectively). There is a spike in Fig. 1 during conditioning at ~6 h, which was caused by the interruption of the conditioning operation for measuring EIS, CV, and LSV. The curves at 0 time, "fresh", were also added to the figures for comparison. These "fresh" values were obtained by measuring a new sample that had not undergone any conditioning. Clearly, after conditioning the electrochemical active area increased, and the membrane resistance (high-frequency intercept) and polarization resistance (the difference between the low- and high-frequency intercepts) decreased. Based on the impedance spectra, membrane resistance (R_{el}), charge transfer resistance (R_{ct}), and mass transfer resistance (R_{mt}) can be extracted using the equivalent circuit depicted in Fig. 5, where CPE represents the constant phase element. The simulated parameters are listed in Table 1.

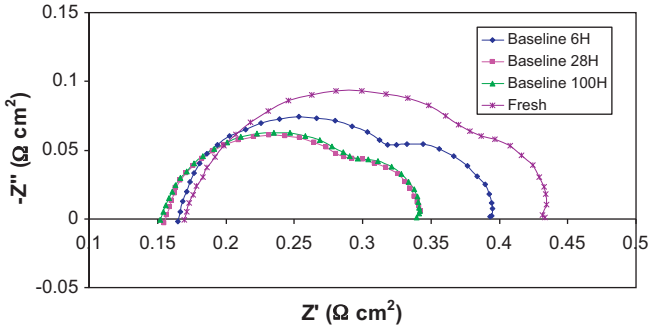

Fig. 2. Comparison of EIS curves at different times during baseline conditioning.

Table 1
Parameters extracted from impedance spectra using the equivalent circuit depicted in Fig. 5.

Accelerated conditioning operation	R_{el} (Ω cm^2)	R_{ct} (Ω cm^2)	R_{mt} (Ω cm^2)	Accelerated conditioning operation	R_{el} (Ω cm^2)	R_{ct} (Ω cm^2)	R_{mt} (Ω cm^2)
Fresh	0.17	0.225	0.045	Baseline 6H	0.165	0.178	0.045
Baseline 28H	0.155	0.148	0.04	Baseline 100H	0.152	0.148	0.04
50 °C	0.167	0.212	0.045	0.6–0.3 V, 20 s	0.157	0.235	0.05
70 °C	0.165	0.178	0.045	0.6–0.3 V, 60 s	0.157	0.152	0.03
90 °C	0.16	0.135	0.024	0.6 V–0.3 V, 5 min	0.169	0.155	0.032
0.6–0.3 V	0.157	0.152	0.03	Short circuit	0.152	0.175	0.043
0.6–0.3 V–OCV	0.157	0.175	0.038	Hot water circulation	0.191	0.268	0.051
Sequential cycling	0.152	0.16	0.04	Hydrogen pumping	0.17	0.19	0.041

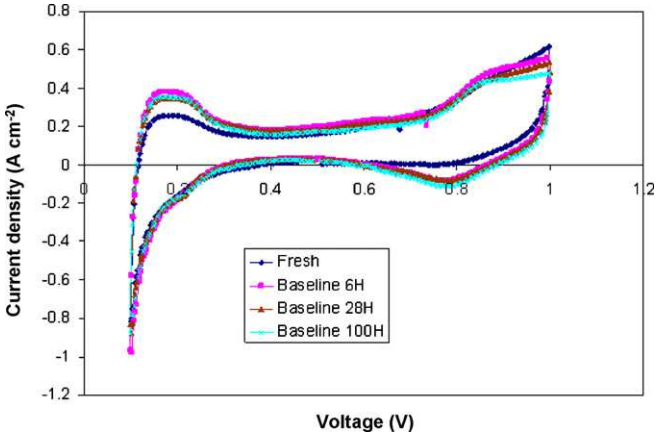

Fig. 3. Comparison of CV curves at different times during baseline conditioning.

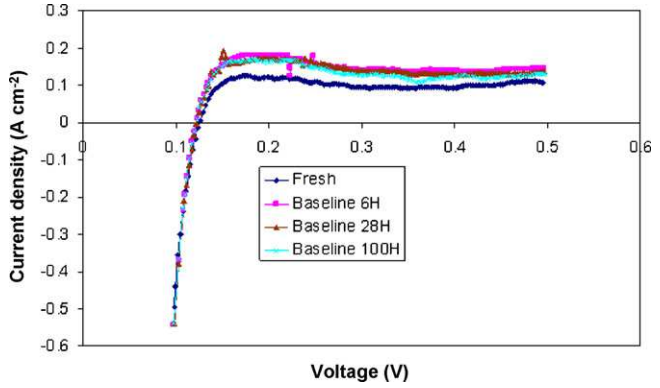

Fig. 4. Comparison of LSV curves at different times during baseline conditioning.

The observed phenomena can be explained by the following possible theories [2]:

(1) Increase in the electrochemical active area of the catalyst: this is achieved by the removal of impurities introduced during the process of manufacturing the MEA and the fuel cell stack, and the activation of a catalyst that does not participate in the reaction.

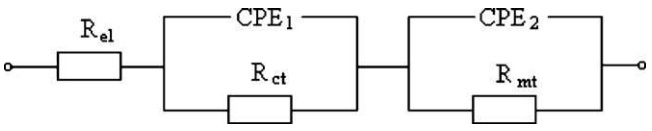

Fig. 5. Equivalent circuit of a resistor and a Voigt's structure in series with capacitors replaced by CPE.

(2) Membrane "break-in": one such theory is that the membranes may include catalyst residue that hinders their performance. Another is that the membranes are initially dry, hindering the cell performance until the membranes hydrate during the incubation period (indicated by the decrease in membrane resistance).
(3) Decrease in charge transfer resistance: the initial performance of a new MEA with Nafion-bonded electrodes usually improves with time, as the electrolyte contained in the electrodes needs hydration to ensure the passage of hydrogen ions.
(4) Decrease in mass transfer resistance: conditioning creates more transfer passages for reactants to the catalyst.

As seen in Fig. 4, hydrogen crossover increases slightly over time compared with the fresh sample. However, the increase is insignificant.

3.2. Effect of temperature

The temperature effect is obtained by comparing the performance after 6 h of conditioning at 50, 70, and 90 °C. Fig. 6 shows the time dependence of current at 0.6 V during 6 h of conditioning at different temperatures. As can be seen, cell performance increases with increasing temperature. For all the temperatures, a similar increasing trend in performance is observed within 6 h, but this time is apparently not enough for the cells to completely reach their best performance. For example, in the baseline case, 20 h of operation is needed. Nevertheless, the greatest performance increase occurs at the very beginning (i.e., 1–2 h). Qi and Kaufman [9] also found that under elevated temperature, the current density at certain cell voltages could be doubled after activation and the activation could be completed extremely quickly, with most of it achieved in the first few minutes.

After 6 h of operation at 0.6 V at different temperatures, EIS, CV, and LSV were measured. The results of CV and EIS are compared in Figs. 7 and 8, respectively. Evidently, after conditioning at different temperatures the electrochemical active area increases (relative to the fresh sample, the electrochemical active area increases by

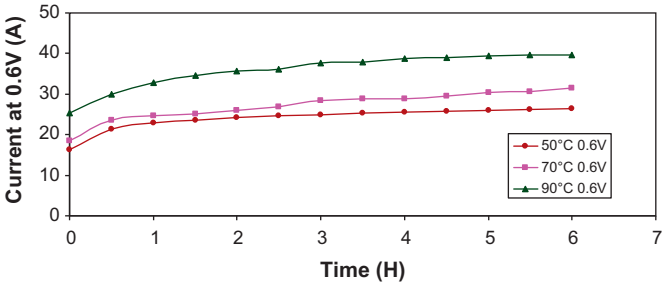

Fig. 6. Comparison of current–time curves at 0.6 V conditioned at different temperatures.

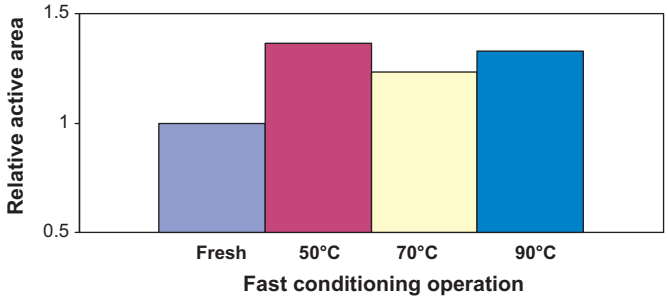

Fig. 7. Comparison of relative active area derived from the CV curves after conditioning at 0.6 V for 6 h at different temperatures. The relative active area of the fresh sample is 1.

1.4, 1.2, and 1.3 times for 50 °C, 70 °C, and 90 °C, respectively). Due to ionomer hydration and catalyst activation, the membrane and polarization resistances decrease, as demonstrated in Fig. 8. Further, according to the simulated impedance parameters listed in Table 1, R_{el}, R_{ct}, and R_{mt} all decrease with increasing temperature. It has been proposed that the activation process increases catalyst utilization by opening many "dead" regions in the catalyst layer. Even when a proton conductor such as Nafion is mixed into a catalyst layer to make it conduct protons in three dimensions, many of the catalyst sites are not available for reaction, for various reasons: (1) the reactants cannot reach the catalyst sites because the latter are blocked, (2) Nafion near these catalyst sites cannot be easily hydrated, or (3) ionic or electronic continuity is not established with these sites. When a fuel cell is operated at elevated temperature and pressure, many of these "dead" regions are "opened" and then become active [9].

With increasing temperature, hydrogen crossover slightly increases due to faster diffusion of hydrogen at higher temperatures.

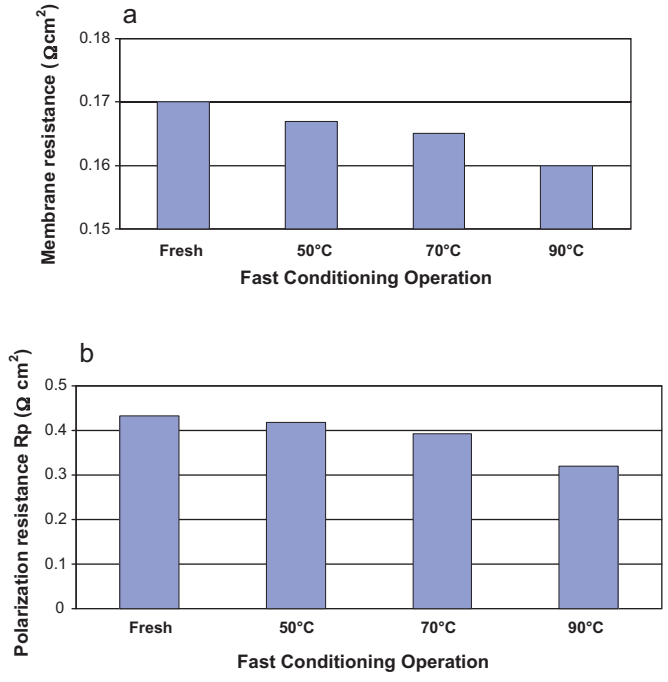

Fig. 8. Comparison of (a) high-frequency resistance (b) polarization resistance derived from EIS curves after conditioning at 0.6 V for 6 h at different temperatures.

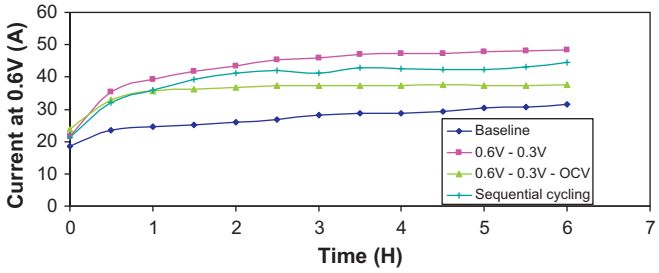

Fig. 9. Comparison of current–time curves at 0.6 V for different cycling steps.

3.3. Effect of cycling steps

The effect of cycling steps was evaluated by comparing the performance after 6 h of conditioning using 2, 3, and more cycling steps. Fig. 9 shows the time dependence of current at 0.6 V during 6 h of conditioning for different cycling steps. As can be seen, any potential cycling operation helped to activate the cell, and cycling between 0.6 V and 0.3 V achieved the best performance within 6 h. In other words, neither OCV relaxation nor cycling with more steps was much help in conditioning the cell. Similar to results from previous tests, the greatest performance increased occurred at the very beginning of conditioning.

After 6 h of conditioning under different cycling steps, EIS, CV, and LSV were measured. Results from CV are compared in Fig. 10, and results from EIS are listed in Table 1. Fig. 10 shows that after conditioning under different potential cycling steps, the electrochemical active area increased, especially for sequential cycling. Compared with the results for a fresh sample, R_{el}, R_{ct}, and R_{mt} all decreased in the three cases. It is generally believed that the membrane hydration level, the number of proton conduction channels, and the catalyst layer porosity continued to increase during the conditioning period. According to Fig. 10, as the number of cycling steps increases, more active area can be obtained. However, this trend does not exactly match the trend in resistance changes as observed from EIS; these activations are effective for improving one factor but may not be effective for improving other factors that affect cell performance. The ultimate performance improvement will be determined by the combined effects of all factors. For LSV, there was no significant change in hydrogen crossover.

3.4. Effect of cycling frequency

The effect of cycling frequency was determined by comparing the performance after 6 h of conditioning under different cycling

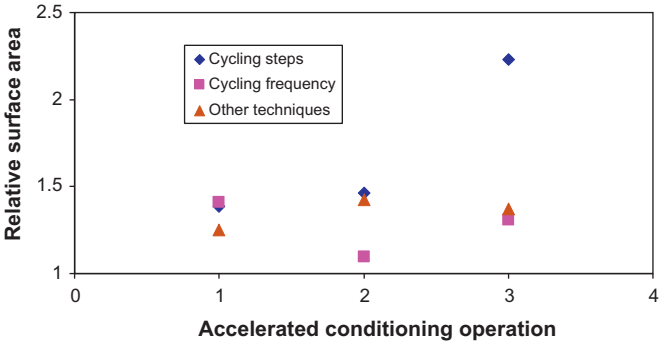

Fig. 10. Comparison of the relative active area derived from the CV curves after conditioning with different conditioning operations (♦) Cycling steps (1:0.6 V–0.3 V; 2: 0.6 V–0.3 V–OCV; 3: Sequential cycling). (■) Cycling frequency (1:0.6 V–0.3 V 20 s; 2: 0.6 V–0.3 V 60 s; 3: 0.6 V–0.3 V 5 min). (▲) Other techniques (1: hot water circulation; 2: short circuit; 3: hydrogen pumping).

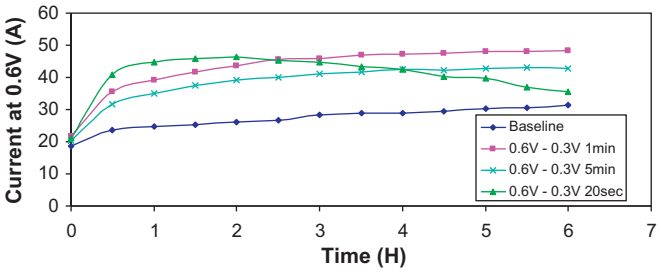

Fig. 11. Comparison of current–time curves at 0.6 V for different cycling frequencies.

frequencies. Fig. 11 shows the time dependence of current at 0.6 V during 6 h of conditioning with different cycling frequencies. As can be seen, within 2 h, the higher the cycling frequency, the more efficiently the cell was activated; at a high frequency of 20 s, the cell reached its best performance within 2 h, followed by performance degradation, whereas for frequencies of 1 min and 5 min, at least 6 h of activation process were needed. At this moment, it is difficult to give an explanation for the effect of frequency. As all the measurements were taken after 6 h of operation, we are unable to track the changes during these 6 h. While other cells are still in the process of conditioning, the cell at a frequency of 20 s has started to degrade within 6 h. We may assume that high frequency works more effectively to improve the electrochemical active area of the catalyst or create the pathways for protons. Furthermore, it is predicted that the cell with potential cycling at a high frequency will have a fast degradation rate.

After 6 h of operation at 0.6 V under different cycling frequencies, EIS, CV, and LSV were measured. The CV results are compared in Fig. 10 and the EIS results are listed in Table 1. For all cases, after conditioning under different cycling frequencies, the electrochemical active area increased. From Table 1 we can see that R_{el}, R_{ct}, and R_{mt} all decreased, except at 20 s. In this case, the increases in R_{ct} and R_{mt} are attributable to degradation after 2 h. Compared with the situation at a frequency of 1 min although conditioning at a low frequency for 5 min yielded a high ECSA, it resulted in high resistance for the membrane and polarization. The lower cell performance for a low frequency of 5 min was a result of the combined factors. For LSV, there was no significant change in hydrogen crossover within such a short time of operation.

3.5. Other methods

Other methods investigated in this report include short circuit, hot water circulation, and hydrogen pumping. The principle of hydrogen pumping is to improve PEM fuel cell performance by moving hydrogen from one side of the membrane to the other. As a result of this process, electrode catalyst utilization is increased and MEA performance is improved [4]. This is achieved by reducing the overpotential of oxygen reduction. The reduction in overpotential is thought to be due to changes in the porosity and tortuosity of the catalyst layers when H_2 evolves from them, leading to an increase in the number of reactant–catalyst–electrolyte 3-phase sites. Hot water circulation was chosen, as it was believed that the Nafion in the MEA could achieve complete hydration (including the Nafion membrane and the Nafion in the CL), leading to enhanced MEA performance. Hot water circulation might also help to open some "dead" regions in the CL [17].

These methods were compared for 0.5 h of operation. Compared with the baseline figures, these methods could activate the cell to a certain extent within 0.5 h. Cell performance was improved in this order: short circuit, hydrogen pumping, and hot water circulation.

After 0.5 h of operation under different conditions, EIS, CV, and LSV were measured. The CV results are compared in Fig. 10, and the EIS results are listed in Table 1. It can be seen that after conditioning under different circumstances, the electrochemical active area increases greatly, especially for the short circuit and hydrogen pumping situations. The short circuit not only achieves the largest active area, but also achieves the smallest membrane and charge transfer resistances (while not contributing to increases in the mass transfer passages), as seen in Table 1. Hydrogen pumping can greatly reduce the charge transfer resistance, but does not contribute to improving the membrane conductivity and increasing the mass transfer paths. Hot water circulation achieved (i) the least active area increase and (ii) an increase in membrane and polarization resistances, probably due to flooding issues.

4. Concluding remarks

This report investigated various methods and factors to condition a PEM fuel cell. The conditioning times and electrochemical properties after conditioning are compared. It is worth noting that these comparisons are based on the Gore CCM. Depending on the type of MEA components, the actual conditioning time and properties may vary. According to our results: higher temperature is more effective to obtain high performance; OCV relaxation and more cycling steps are not very helpful in accelerating the process; higher cycling frequency may reduce the activation time, but is soon followed by degradation; and the short circuit method seems very effective to condition the cell in a very short time. However, applying all these stressors to condition the cell strongly affects the microstructures of the conditioned MEA, which in turn will strongly affect the long-term behaviour and durability of the cell, as MEA nanomaterial degradation is heavily history-dependent. For example, although short circuits can condition the cell in a very short time, we do not know how this will affect the cell's durability without a long-term durability test. The effect of conditioning on cell durability may be studied in our future work.

References

[1] Z. Xu, Z. Qi, C. He, A. Kaufman, J. Power Sources 156 (2006) 315–320.
[2] X.Z. Yuan, S. Zhang, J.C. Sun, H. Wang, J. Power Sources 196 (2011) 9097–9106.
[3] M. Murthy, N.T. Sisofo III, C.A. Baczowski, Method and device to improve operation of a fuel cell, US 2006/0166051 A1 (2006).
[4] C. He, Z. Qi, M. Hollett, A. Kaufman, Electrochem. Solid-State Lett. 5 (2002) A181–A183.
[5] W. Bi, Electrochem. Solid-State Lett. 10 (2007) B101–B104.
[6] J. Shan, X., Yan, X., Sun, Z., Hou, P., Qi, P. Ming, A fast activation method for a fuel cell stack, Chinese Patent, 201010010014.3 (2010).
[7] T.W. Lim, S.H. Kim, S.Y. Ahn, B.K. Hong, B.K. Ahn, System and method for activating fuel cell, US 2010/0129689 Al, 2010.
[8] F.-B. Weng, B.-S. Jou, A. Su, S.H. Chan, P.-H. Chi, J. Power Sources 171 (2007) 179–185.
[9] Z. Qi, A. Kaufman, J. Power Sources 111 (2002) 181–184.
[10] Z. Qi, A. Kaufman, J. Power Sources 114 (2003) 21–31.
[11] Z. Qi, A. Kaufman, Activation of electrochemical cells with catalyst electrodes, US Patent 6,805,983 (2004).
[12] C. He, Z. Qi, A. Kaufman, Electrochemical method to improve the performance of H_2/air PEM fuel cells and direct methanol fuel cells, US Patent 6,730,424 (2004).
[13] Z. Xu, Z. Qi, J. Power Sources 156 (2006) 281–283.
[14] H.H. Voss, R.H. Barton, M. Sexsmith, M.J. Turchyn, Conditioning and Maintenance Methods for Fuel Cells, Ballard Power Systems Inc., CA 2429598 A1, 2003.
[15] C. Eickes, P. Piela, J. Davey, P. Zelenay, J. Electrochem. Soc. 153 (2006) A171–A178.
[16] K. Palanichamy, A.K. Prasad, S.G. Advan, Off-line conditioning of PEM fuel cell membrane electrode assembly (MEA), ECS Abstract, http://www.electrochem.org/meetings/scheduler/abstracts/214/1091.pdf (accessed 24.03.11).
[17] Z. Qi, A. Kaufman, J. Power Sources 109 (2002) 227–229.
[18] USFCC single cell test protocol, Available at http://www.fchea.org/core/import/PDFs/Technical%20Resources/MatComp%20Single%20Cell%20Test%20Protocol%2005-014RevB.2%20071306.pdf (accessed 24.03.11).